Hindawi Publishing Corporation
ISRN Condensed Matter Physics
Volume 2014, Article ID 763401, 7 pages
http://dx.doi.org/10.1155/2014/763401

Research Article

Theoretical Investigations of Structural Phase Transitions and Magnetic, Electronic and Thermal Properties of DyNi: Under High Pressures and Temperatures

Pooja Rana and U. P. Verma

School of Studies in Physics, Jiwaji University, Gwalior 474 011, India

Correspondence should be addressed to Pooja Rana; poojafizix@yahoo.com

Received 9 September 2013; Accepted 17 December 2013; Published 4 February 2014

Academic Editors: H.-D. Yang and A. D. Zaikin

Present work is influenced by the requirement of investigation of rare earth intermetallics due to the nonavailability of theoretical details and least information from experimental results. An attempt has been made to analyse the structural, electronic, magnetic and thermal properties of DyNi using full potential linear augmented plane wave method based on density functional theory. DyNi differs from other members of lanthanides nickelates as in ground state it crystallizes in FeB phase rather than orthorhombic CrB structure. The equilibrium lattice constant, bulk modulus, and pressure derivative of bulk modulus are presented in four polymorphs (FeB, CrB, CsCl and NaCl) of DyNi. At equilibrium the cell volume of DyNi for FeB structure has been calculated as 1098.16 $Bohr^3$ which is comparable well with the experimental value 1074.75 $Bohr^3$. The electronic band structure has been presented for FeB phase. The results for thermal properties, namely, thermal expansion coefficient, Gruneisen parameter, specific heat and Debye temperature at higher pressure and temperatures have been reported. The magnetic moments at equilibrium lattice constants have also been tabulated as the rare earth ions associated with large magnetic moments increase their utility in industrial field for the fabrication of electronic devices due to their magnetocaloric effect used in magnetic refrigeration.

1. Introduction

Because of the technological importance, the rare earth compounds have attracted interest of the experimental as well as the theoretical scientists during past decade. The rare earth elements on combining with transition metals show peculiar characteristics like good oxidation resistance and excellent strength [1]. Due to large magnetic moments and magnetocaloric effect (MCE) they also have applications in the fabrication of permanent magnets, magnetostrictive devices, magnetooptical recorders [2] and magnetic refrigeration [3–10]. These are also taken as first choice for the purpose of hydrogen storage materials [11]. Among all transition metals nickel is one of the promising materials in its pure form and also in alloy form doped with other materials. The structural parameters of some Gadolinium and Dysprosium intermetallics and their related compounds have been reported by Baenziger and Moriarty Jr. [12]. A sample of polycrystalline DyNi was prepared by Tripathy et al. [13] and its magnetocaloric effects have been studied on varying temperature scale by using powder X-ray diffractogram. Later, the magnetic properties of lanthanides-nickel intermetallic compounds and their relative hydrides have been studied by Yaropolov et al. [3, 4].

Thus, it is clear from the above paragraph that some attention has been paid on the studies of magnetic properties of rare earth nickel compounds and its hydrides, whereas till so far no attention has been paid on the properties like electronic, mechanical, thermal, and so forth. Realising the need of theoretical exploration of rare earth compounds, we focus our attention around rare earth nickelates (RNi) to explain them on the basis of earlier mentioned properties by using first principles approach.

DyNi compound has attracted much attention because of their magnetic and extraordinary magneto-elastic and magnetocaloric properties and its uses in the fabrication of

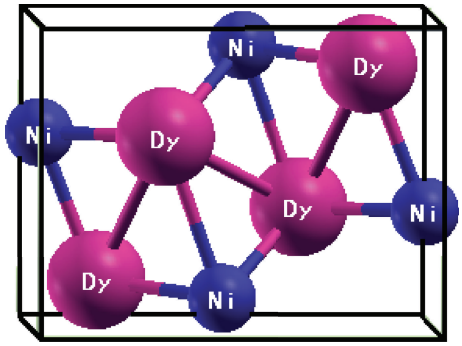

Figure 1: Cell structure of DyNi in FeB phase.

Table 1: Lattice coordinates (x, y, z) in FeB. CrB, CsCl, and NaCl phases of DyNi.

Atoms	Lattice coordinates		
	x	y	z
		FeB phase	
Dy	0.179	0.250	0.132
Ni	0.035	0.250	0.609
		CrB phase	
Dy	0.000	0.146	0.250
Ni	0.000	0.440	0.250
		CsCl/NaCl phases	
Dy	0.000	0.000	0.000
Ni	0.500	0.500	0.500

materials in magnetic refrigerators [14–16]. Moreover, this compound is also having peculiarities of the interaction with hydrogen and ability to absorb up to 3 atoms/formula units (fu).

The goal of present communication is to report lacking bulk properties of DyNi using first principles study, namely, magnetic, electronic, and structural properties. The structural studies of DyNi has been reported in FeB, CrB, CsCl and NaCl structures. The effects of high pressure and high temperature on the electronic, magnetic, and thermal properties of the compound have also been reported. Methodology of the study, results, and discussions and conclusions are given in subsequent sections.

2. Computational Methodology

In ground state DyNi crystallizes in orthorhombic structure of FeB with space group (62-Pnma) [6]. The primitive cell structure of DyNi in FeB phase is shown in Figure 1. The structure contains two pairs of Fe as well as Ni atoms.

The DyNi has been investigated using full potential linear augmented plane wave (FP-LAPW) method within the frame work of density functional theory (DFT) [17, 18] as implemented in code Wien2k [19]. The generalized gradient approximation (GGA) for the exchange-correlation interaction given by Perdew, Burke, and Ernzerhof (PBE) [20] has been used. In this method, the basis set inside each muffin-tin sphere is split into two parts: core subset and valence subset. The states under core region are treated as being spherically symmetric of the potential and are assumed to have a spherically symmetric charge density confined inside the muffin-tin spheres. The valence part is treated within a potential which is expanded into spherical harmonics up to $l = 4$. The valence wave functions inside the spheres are expanded up to $l_{\max} = 8$. The energy convergence criterion of electronic self-consistency is chosen as 10^{-4} Ry whereas charge convergence as 10^{-3} e^-. At ambient conditions DyNi crystallizes in orthorhombic FeB structure having space group 62-Pnma [21]. The primitive cell structure of DyNi in FeB phase is shown in Figure 1. From the inspection of Figure 1 it indicates that the structure contains two pairs of Fe as well as Ni atoms. Each Dy atom is shared by four tetrahedral where Dy atoms are placed at the corners sharing by the corners and edges with other tetrahedral. The calculations are made to relax the lattice coordinates for the atoms Dy and Ni in all the four structures. Atomic positions in four different structures are given in Table 1. The energy that separates the valence states from core states has been taken as −6.0 Ry. The k-points within first Brillouin zone of the reciprocal space have been chosen to be 2500 for DyNi in FeB structure.

The electronic structure has also been computed using PBE-GGA. Since knowledge about thermodynamical properties in the fabrication of modern devices is essential, therefore, the effects of temperature and pressure have also been studied related to DyNi based on quasiharmonic Debye model as implemented in Gibbs Program [22].

Further rare earth intermetallics were generally found to be crystallizing in three other crystal structures, namely, CsCl, NaCl, and CrB. Hence, analysis of the stability of DyNi in these three phases has also been reported. The k-points within first Brillouin zone of the reciprocal space have been chosen as 1331, 1331, and 1000, respectively, for CrB, CsCl, and NaCl phases.

3. Results and Discussions

3.1. Structural Properties. The total energy has been calculated corresponding to different cell volumes of FeB, CrB, CsCl, and NaCl phases of DyNi and fitted to the Murnaghan equation of state [15]. During simulations it has been noticed that the total energy and volume of the unit cell of FeB phase are two times as compared to those of CrB phase while they are four times of the total energy and volume of the unit cell of CsCl and NaCl phases. The cause behind this is that the unit cell of FeB phase is made up of 4 primitive cells, while CrB phase contains 2 and CsCl and NaCl phases contain single primitive cell. In order to normalise the energy as well as the volume of all four phases, supercells have been generated for CrB phase, and CsCl and NaCl phase of size of $2 \times 1 \times 1$ and $2 \times 2 \times 1$, respectively. The results of the supercell calculations are two and four times to their respective unit cells. The four optimized plots are depicted in Figure 2. It is evident from this plot that ground state phase of DyNi is FeB structure and its curve for CrB phase is found to be very close to ground state. The CsCl and NaCl optimization curve lies

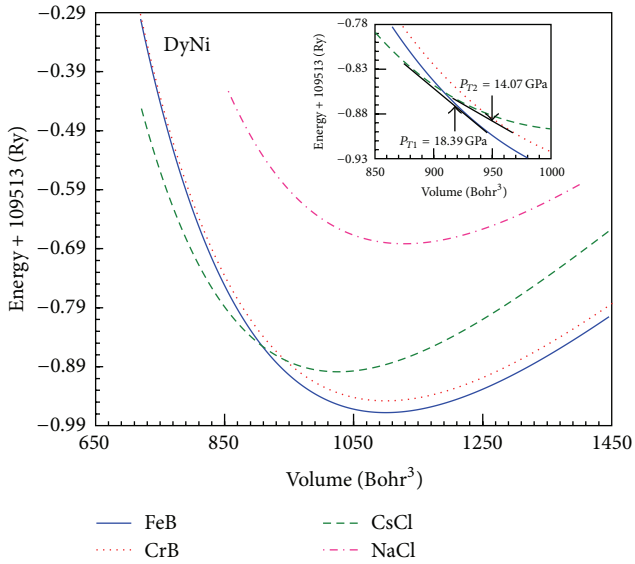

FIGURE 2: Plots of total energies as function of cell volumes in FeB, CrB, CsCl and NaCl phases of DyNi.

above ground state curve. The equilibrium volume in CrB and NaCl structure are more than the ground state equilibrium volume while it is less in the case of CsCl phase. Looking into plots phase transitions are noticeable from FeB to CsCl and CrB to CsCl phase. Details about the transition pressures are given under section phase transition. The equilibrium lattice constants, and bulk modulus and its pressure derivatives obtained after fit are listed in Table 2 along with earlier reported experimental results [6].

In our present study the values of lattice parameters for FeB structure have been computed as $a = 13.435$ Bohr, $b = 7.959$ Bohr, and $c = 10.27$ Bohr which is quite agreeable with the experimental lattice constants $a = 13.27$ Bohr, $b = 7.89$ Bohr, $c = 10.28$ Bohr. For CrB structure $a = 7.085$ Bohr, $b = 19.424$ Bohr, and $c = 7.859$ Bohr, for CsCl structure $a = 6.366$ Bohr, and for NaCl structure $a = 10.409$ Bohr. In these structures of DyNi, experimental results are not available.

3.1.1. Phase Transitions. The aim of studying DyNi in four structures is to look for possible structural phase transformations from one phase to another. Figure 2 reveals the fact that optimization curves in FeB and CrB phase are very close to each other near equilibrium. With the increase in pressure near 57 GPa both the curves overlap each other. The optimization curve in CsCl phase crosses to the optimization curves in FeB and CrB phases. The ground state FeB phase transforms to CsCl phase at pressure $P_{T1} = 18.39$ GPa while CrB phase shows structural phase transitions at $P_{T2} = 14.07$ GPa. The NaCl phase shows separate optimization curve, that is, there is no interconnection between NaCl and other phases.

3.2. Electronic Properties. The self-consistent electronic band structures in spin-up and spin-down channels of DyNi for FeB phase are presented in Figure 3. In both the channels DyNi shows metallic nature. In order to explicate band structures, total and partial densities of states (DOS) for Dy and Ni atoms are shown in Figure 4. Total DOS of DyNi and atoms Dy and Ni are drawn in Figure 4(a). In both the spins total DOS of DyNi is less than four times the sum of atomic total DOS because of the reason that FeB structure of DyNi contains 4 Dy and 4 Ni atoms. This difference shows the presence of some itinerant electrons which are free to move anywhere within the compound.

In the partial DOS of atom Dy major contribution in DOS is from f-states. In spin-up channel peaks are concentrated in the range -2.0 to -4.0 eV (below Fermi level) while in spin-down channel f-states overlap Fermi level completely from -0.5 to 1.4 eV. Negligible contribution of other electron states, namely, s-states, p-states, and d-states is seen in both the channels. In case of Ni atoms, it can be noticed that DOS plots for spin up and spin down channels are nearly the same for all the electrons and major contribution is from d-states between -3.0 eV and Fermi energy level.

3.3. Thermal Properties. Lattice dynamics is an important aspect to study properties of materials. It concerns the vibrations of the atoms about their mean position. These vibrations are entirely responsible for thermal properties, namely, heat capacity, thermal expansion, entropy, and so forth. Thermal properties of DyNi have been quite useful from different aspects of magneto-caloric effect. As the temperature and pressure of the material vary, it affects the density of the material which indicates the thermal expansion/contraction within the material leading to important and interesting results. Obtained thermodynamical results are listed in Table 3. To compute reported properties temperature range has been varied from 0 to 1000 K and pressure was taken between 0 and 20 GPa. Various parameters like thermal expansion coefficient (α), Gruneisen parameter (γ), debye temperature (θ_D), and specific heat (C_P and C_v) as a function of pressures/temperatures have been presented in Figure 5. Their analysis is presented in the following sections.

3.3.1. Thermal Expansion Coefficient. Effect of temperature on thermal expansion coefficient (α) has been analysed and shown in Figure 5(a) at hydrostatic pressure $P = 0$, 8, and 16 GPa. Figure 5(a) shows that thermal expansion increases with the increase in temperature up to 100 K after that it attains saturation. At this particular temperature, expansion coefficient decreases with the increase in pressure.

3.3.2. Gruneisen Parameter. Gruneisen Parameter (γ) is the next parameter of solids related with the effect in lattice vibrations and gives details about vibrational anharmonicity. The variation of γ with respect to pressure has been depicted in Figure 5(b) for three different temperature ($T = 0$ K, 500 K and 1000 K). The behaviour of this parameter is that it decreases with increase in pressure at constant temperature while at constant pressure it increases as the temperature increases.

3.3.3. Specific Heat and Debye Temperature. The amount of energy given to lattice vibrations in the crystalline solids is

Table 2: Optimized results for equilibrium lattice constants "a" (Bohr), a/c ratio, unit cell volumes V_0 (Bohr^3), and bulk modulus B_0 (GPa) and its first order pressure derivative.

Structure	Results	Lattice constants			a/c ratio	V_0	B_0	B_0'
		a	b	c				
FeB	Present work	13.44	7.96	10.27	1.31	1098.16	72.05	4.63
	Expt. [6]	13.27	7.89	10.28	1.29	1074.75		
CrB	Present work	7.09	19.42	7.86	0.90	1081.55*	71.61	4.18
CsCl	Present work	6.37			—	1031.96*	74.33	4.68
NaCl	Present work	10.41			—	1127.80*	66.92	4.65
		Transition pressure P_T (GPa)						
P_{T1} (FeB $\rightarrow$ CsCl)		Present work		18.39 GPa		Expt.	—	
P_{T2} (CrB $\rightarrow$ CsCl)		Present work		14.07 GPa		Expt.	—	

*V_0 corresponds to supercell volume.

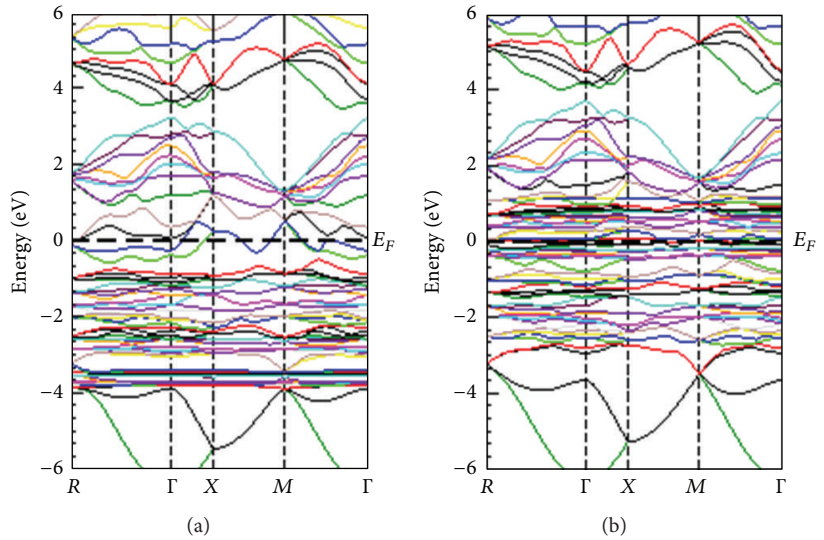

Figure 3: Band Structures of DyNi in FeB phase at ambient pressure and temperature (a) spin up channel and (b) spin down channel.

Table 3: Calculated results for thermodynamical properties in FeB structure of DyNi.

Properties	$P = 0$ GPa $T = 0$ K	$P = 0$ GPa $T = 300$ K
Thermal expansion coefficient α (10^5/K)	0	1.43
Specific heat at constant volume C_v (J/mol K)	0	49.32
Specific heat at constant pressure C_p (J/mol K)	0	49.75
Gruneisen parameter γ	2.04	2.051
Debye temperature θ_D (K)	144.67	143.19
Entropy S (J/mol K)	0	103.55

the dominant contribution to the specific heat which is a measure of degrees of freedom to absorb energy. The specific heats as a function of temperature at ambient pressure are shown in Figure 5(c). The plots show standard trend of heat capacity and its highest value (~48 J/mol K) is approximately twice of the value of $3R$ (=24.9 J/mol K). Here R is universal gas constant. The increased value in heat capacity may be correlated to the fact that the large value of the magnetic moments corresponding to the higher value of temperature becomes ordered. The Debye temperature as a function of pressure is presented in Figure 5(d) at $T = 0$, 500, and 1000 K. The Debye temperature varies nonlinearly with the increase in pressure and separation of the curves increases with the increase in temperature.

3.4. Magnetic Properties. Magnetic moments of interstitial region, atoms Dy and Ni, total magnetic moment (M_M) and total M_M/formula unit (M_M/fu) for FeB, CrB, CsCl, and NaCl phases of DyNi are given in Table 4. The interstitial magnetic moments in FeB, CrB, and CsCl phases are positive while it is negative for NaCl phase. The magnetic behaviour of atom Dy is nearly identical in all the phases of DyNi as its magnetic moments are obtained ~4.6 μB. The electronic configuration

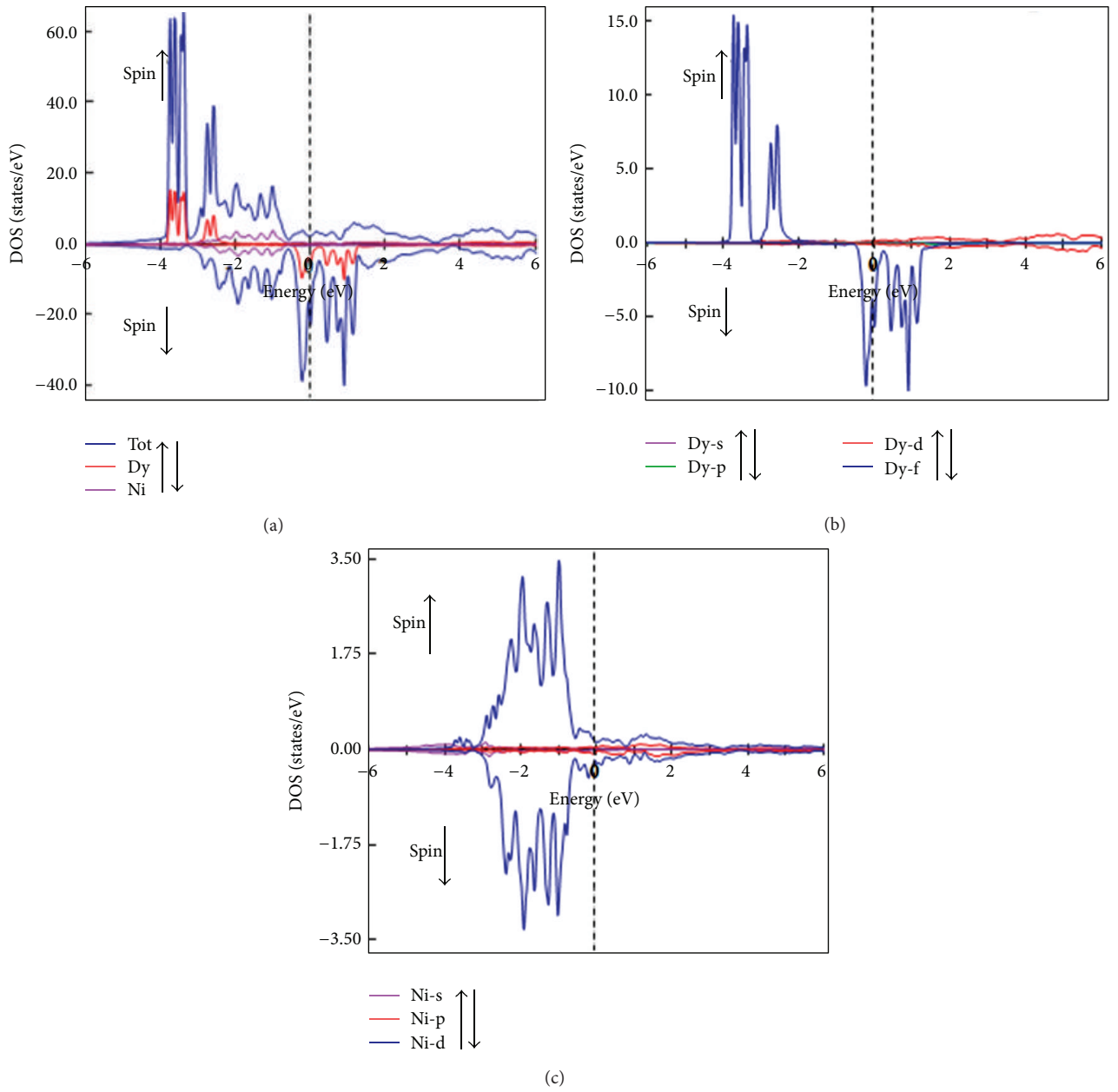

Figure 4: Total and partial density of states for DyNi in FeB phase.

Table 4: Magnetic moments of interstitial region, atoms Dy and Ni, total magnetic moment (M_M), and total M_M/formula unit (M_M/fu) for FeB, CrB, CsCl, and NaCl phases of DyNi.

Sites	Magnetic moment (μB)			
	FeB	CrB	CsCl	NaCl
Interstitial	0.30168	0.18221	0.05911	−0.01504
Atom Dy	4.63309	4.60257	4.66920	4.71424
Atom Ni	0.01003	0.02365	0.06351	0.16738
Total M_M	18.87416	9.34005	4.79181	4.86658
Total M_M/fu	4.71854	4.67002	4.79181	4.86658

of Dy is [Xe] $4f^9$, $5d^1$, and $6s^2$. It seems that the magnetic moment of Dy is intimately related to the highly localized 4f electrons. Similarly, behaviour of atom Ni is identical in all four phases. The total magnetic moment per formula unit is ~4.7 μB in all phases. The total magnetic moment for the complete DyNi in FeB phase is found to be 18.87 μB; in CrB phase it is 9.34 μB while in CsCl and NaCl phases it is around 4.8 μB. The reason behind this is that FeB phase contains 4 primitive cells per unit cell and CrB phase includes 2 primitive cells per unit cell.

4. Conclusions

Present paper includes *ab initio* study of the structural and magnetic properties of DyNi alloy using FP-LAPW method. The GGA is opted to perform all the calculations

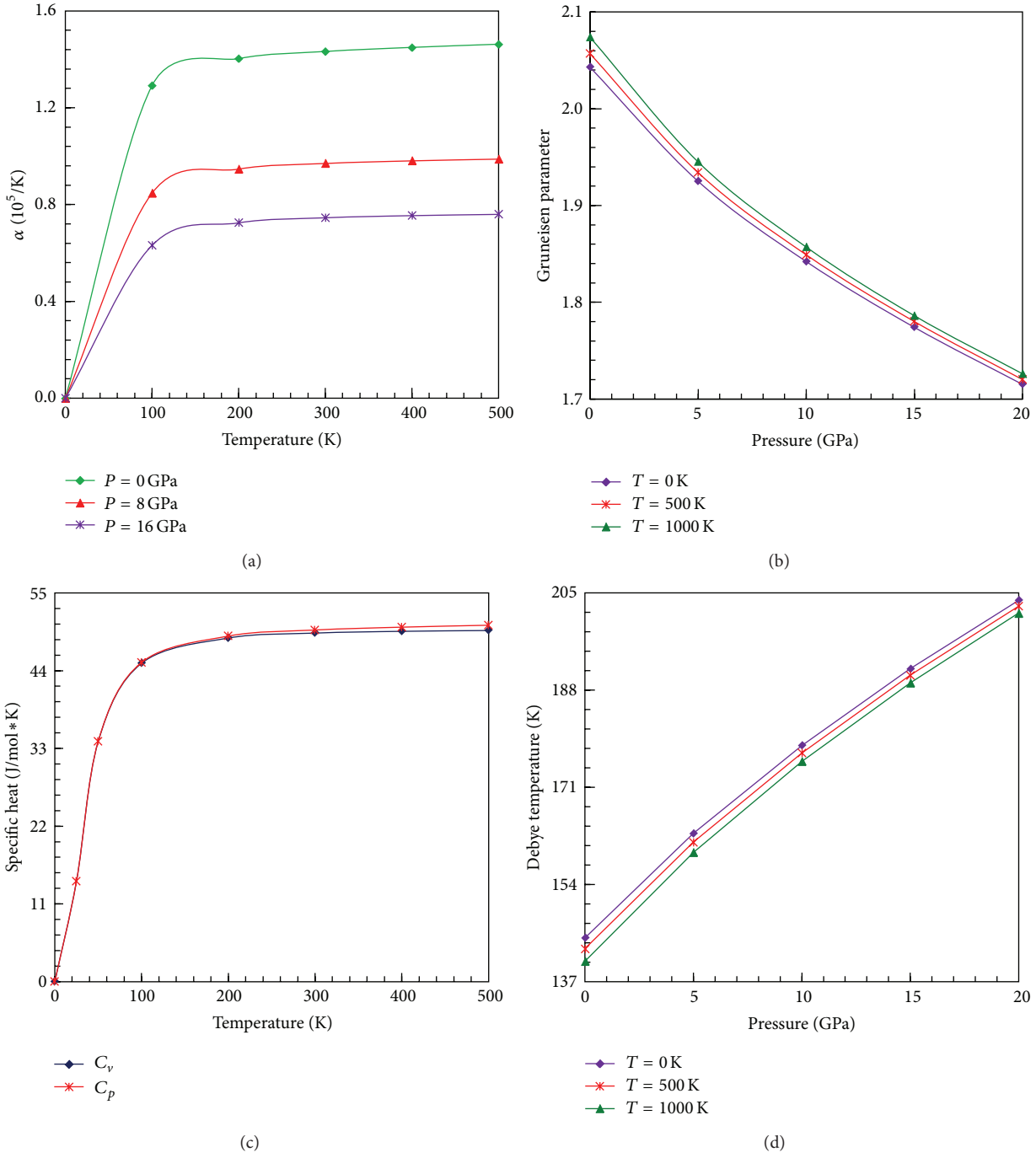

FIGURE 5: Thermodynamical parameters: (a) thermal expansion coefficient α, (b) Gruneisen parameter (γ), (c) specific heats C_v and C_p, and (d) Debye temperature θ_D.

related to exchange-correlation functional. The structural phase transformations phase may enhance their physical properties. The optimized results for equilibrium lattice constants, a/c ratio for stabilisation of orthorhombic FeB phase, unit cell volumes, and bulk modulus and its first order pressure have been reported. The electronic band structure and corresponding DOS plots show metallic nature of DyNi in both the channels of spin. Thermal expansion coefficient α, specific heats C_v and C_p, gruneisen parameter γ, Debye temperature θ_D, entropy S, and magnetic moments of DyNi are reported. Only available experimental data about DyNi are lattice constants. The theoretical predictions on structural, electronic, thermal and magnetic properties of DyNi have been reported for the first time. We expect that our present communication will hopefully encourage theoretical researchers and experimentalists to give their attention

to such technically imperative ferromagnetic intermetallic materials.

Conflict of Interests

The authors declare that there is no conflict of interests regarding the publication of this paper.

References

[1] G. H. Caoa, Z. Yua, and A. M. Russell, "The deformation behavior of DyCu ductile intermetallic compound under compression," *Materials Science and Engineering: A*, vol. 528, no. 24, pp. 7173–7177, 2011.

[2] N. H. Duc, "Intersublattice exchange coupling in the lanthanide-transition metal intermetallics," in *Handbook on the Physics and Chemistry of Rare Earths*, K. A. Gschneidner Jr. and L. Eyring, Eds., vol. 24, chapter 163, pp. 339–398, Cryogenic Labora, Hanoi, Vietnam, 1997.

[3] Y. L. Yaropolov, A. S. Andreenko, S. A. Nikitin, S. S. Agafonov, V. P. Glazkov, and V. N. Verbetsky, "Structure and magnetic properties of RNi (R = Gd, Tb, Dy, Sm) and R6M1.67Si3 (R = Ce, Gd, Tb; M = Ni, Co) hydrides," *Journal of Alloys and Compounds*, vol. 509, no. 2, pp. S830–S834, 2011.

[4] R. Mallik, P. L. Paulose, E. V. Sampathkumaran, S. Patil, and V. Nagarajan, "Coexistence of localized and (induced) itinerant magnetism and heat-capacity anomalies in $Gd_{1-x}Y_xNi$ alloys," *Physical Review B*, vol. 55, no. 13, pp. 8369–8373, 1997.

[5] P. L. Paulose, S. Patil, R. Mallik, E. V. Sampathkumaran, and V. Nagarajan, "Ni3d-Gd4f correlation effects on the magnetic behaviour of GdNi," *Physica B*, vol. 223-224, no. 1-4, pp. 382–384, 1996.

[6] E. Gratz, G. Hilscher, H. Sassik, and V. Sechovsky, "Magnetic properties and electrical resistivity of $(Gd_xLa_{1-x})Ni$, $(0 \leqslant x \leqslant 1)$," *Journal of Magnetism and Magnetic Materials*, vol. 54-57, no. 1, pp. 459–460, 1986.

[7] E. Gratz and A. Lindbaum, "Anomalous thermal expansion in Gd-based intermetallics," *Journal of Magnetism and Magnetic Materials*, vol. 177-181, no. 2, pp. 1077–1078, 1998.

[8] D. Paudyal, Y. Mudryk, Y. B. Lee, V. K. Pecharsky, K. A. Gschneidner Jr., and B. N. Harmon, "Understanding the extraordinary magnetoelastic behavior in GdNi," *Physical Review B*, vol. 78, no. 18, Article ID 184436, 2008.

[9] C. A. Poldy and K. N. R. Taylor, "Possible influence of 3d states on the stability of rare earth-rich rare earth-transition metal compounds," *Physica Status Solidi A*, vol. 18, no. 1, pp. 123–128, 1973.

[10] R. E. Walline and W. E. Wallace, "Magnetic and structural characteristics of lanthanide-nickel compounds," *The Journal of Chemical Physics*, vol. 41, no. 6, pp. 1587–1591, 1964.

[11] Y. L. Yaropolov, V. N. Verbetsky, A. S. Andreenko, K. O. Berdyshev, and S. A. Nikitin, "Magnetic properties of the intermetallic compounds RNi (R = Gd, Tb, Dy, Sm) and their hydrides," *Inorganic Materials*, vol. 46, no. 4, pp. 364–371, 2010.

[12] N. C. Baenziger and J. L. Moriarty Jr., "Gadolinium and dysprosium intermetallic phases. I. The crystal structures of DyGa and GdPt and their related compounds," *Acta Crystallographica*, vol. 14, pp. 946–947, 1961.

[13] S. K. Tripathy, K. G. Suresh, R. Nirmala, A. K. Nigam, and S. K. Malik, "Magnetocaloric effect in the intermetallic compound DyNi," *Solid State Communications*, vol. 134, no. 5, pp. 323–327, 2005.

[14] P. Kumar, K. G. Suresh, A. K. Nigam, and O. Gutfleisch, "Large reversible magnetocaloric effect in RNi compounds," *Journal of Physics D*, vol. 41, no. 24, Article ID 245006, 2008.

[15] P. J. von Ronke, D. F. Grangeia, A. Caldas, and N. A. Oliveria, "Investigations on magnetic refrigeration: application to RNi_2 (R = Nd, Gd, Tb, Dy, Ho, and Er)," *Journal of Applied Physics*, vol. 93, p. 4055, 2003.

[16] R. Mondal, R. Nirmala, J. Arout Chelvane, and A. K. Nigam, "Magnetocaloric effect in the rare earth intermetallic compounds RCoNi (R = Gd, Tb, Dy, and Ho)," *Journal of Applied Physics*, vol. 113, p. 17A930, 2013.

[17] P. Hohenberg and W. Kohn, "Inhomogeneous electron gas," *Physical Review*, vol. 136, no. 3B, pp. B864–B871, 1964.

[18] W. Kohn and L. J. Sham, "Self-consistent equations including exchange and correlation effects," *Physical Review*, vol. 140, no. 4A, pp. A1133–A1138, 1965.

[19] P. Blaha, K. Schwarz, G. K. H. Madsen, D. Kvasnicka, and J. Luitz, *WIEN2k, an Augmented PlAne Wave Plus Local Orbitals Program for Calculating Crystal Properties*, Vienna University of Technology, Vienna, Austria, 2001.

[20] J. P. Perdew, K. Burke, and M. Ernzerhof, "Generalized gradient approximation made simple," *Physical Review Letters*, vol. 77, no. 18, pp. 3865–3868, 1996.

[21] M. A. Blanco, E. Francisco, and V. Luaña, "GIBBS: isothermal-isobaric thermodynamics of solids from energy curves using a quasi-harmonic Debye modelComputer Physics Communications," vol. 158, no. 1, pp. 57–72, 2004.

[22] F. D. Murnaghan, "The compressibility of media under extreme pressures," *Proceedings of the National Academy of Sciences of the United States of America*, vol. 30, no. 9, pp. 244–247, 1944.